IEEE Access
Multidisciplinary | Rapid Review | Open Access Journal

Received December 16, 2019, accepted January 15, 2020, date of publication January 20, 2020, date of current version January 28, 2020.

Digital Object Identifier 10.1109/ACCESS.2020.2967846

Genetic Algorithm Based Bilayer PTS Scheme for Peak-to-Average Power Ratio Reduction of FBMC/OQAM Signal

SIYING LV[1], JUNHUI ZHAO[1,2], (Senior Member, IEEE), LIHUA YANG[1], AND QIUPING LI[1]

[1]School of Electronic and Information Engineering, Beijing Jiaotong University, Beijing 100044, China
[2]School of Information Engineering, East China Jiaotong University, Nanchang 330013, China

Corresponding author: Junhui Zhao (junhuizhao@hotmail.com)

This work was supported in part by the National Natural Science Foundation of China under Grant 61661021 and Grant 61971191, in part by the Beijing Natural Science Foundation under Grant L182018, in part by the National Science and Technology Major Project of the Ministry of Science and Technology of China under Grant 2016ZX03001014-006, and in part by the Open Research Fund of National Mobile Communications Research Laboratory, Southeast University under Grant 2017D14.

ABSTRACT Partial transmit sequence (PTS) scheme has been well applied to reduce the high peak-to-average power ratio (PAPR) of the orthogonal frequency division multiplexing (OFDM) signal. However, due to the signal structure differences between the filter bank multicarrier and offset quadrature amplitude modulation (FBMC/OQAM) signal and the OFDM signal, the conventional PTS scheme is not applicable to the FBMC/OQAM signal. Considering the PAPR reduction issue for the FBMC/OQAM signal, this paper proposes a genetic algorithm (GA) based bilayer partial transmit sequence (GA-BPTS) scheme. In order to reduce the computational complexity, the proposed scheme continues to partition each subblock, transforming the single layer structure of the conventional PTS into a bilayer phase factor search structure, and introduces a penalty threshold. Then the suboptimal phase factor vector is obtained by using the GA. Meanwhile, before PAPR reduction processing, aided by the proposed prototype filter which has the better performance of out-of-band attenuation than the PHYDAYS filter, the GA-BPTS scheme can effectively reduce the PAPR of the FBMC/OQAM signal. The simulations have confirmed that the proposed scheme not only provides an excellent PAPR performance but also decreases the computational complexity compared with the conventional PTS scheme.

INDEX TERMS Bilayer partial transmit sequence (PTS), filter bank multicarrier and offset quadrature amplitude modulation (FBMC/OQAM), genetic algorithm (GA), peak-to-average power ratio (PAPR) reduction.

I. INTRODUCTION

Orthogonal frequency division multiplexing (OFDM) is one of the most representative multicarrier modulation (MCM) techniques due to its capability to efficiently cope with frequency selective channels for the upcoming fifth generation (5G) broadband wireless communication [1]–[3]. However, there are some shortcomings spotted for the OFDM system whose adoption is not taken for granted in the 5G, and we shift our attention on the filter bank multicarrier with offset quadrature amplitude modulation (FBMC/OQAM) system [4], [5]. As an heir of the OFDM, the FBMC/OQAM system is derived from a spectrally well-designed prototype filter shaped on each single subchannel [6]. Instead of a fixed rectangular pulse shaping window, the prototype filter of the FBMC/OQAM system can be designed with arbitrarily low side lobe energy to effectively improve the spectral efficiency of the FBMC/OQAM system [7], [8]. Moreover, based on the well-designed prototype filter, FBMC/OQAM system only requires orthogonality for the neighbouring subchannels and therefore has the ability to prevent the asynchronous signals distortion in adjacent bands [9], [10]. Similar to the OFDM system, the high peak-to-average power ratio (PAPR) of the transmitted signal is still unresolved in the FBMC/OQAM system [11]. When FBMC/OQAM signals traveling through some nonlinear devices like the transmit power amplifier, the high PAPR could result in the distortion which can lead to the escalation of bit error rate (BER). Furthermore, the

The associate editor coordinating the review of this manuscript and approving it for publication was Ning Zhang.

detrimental effect may be made on battery lifetime in mobile applications because of the high PAPR [12]. Therefore, it is critical and necessary to pay attention to the issue how to reduce the PAPR for making full use of the technical features in the FBMC/OQAM system.

In view of the similarity between the FBMC/OQAM system and the OFDM system, it is natural for us to explore the PAPR reduction schemes in OFDM system and therefore employ them to reduce the high PAPR in FBMC/OQAM system [13]. The clipping technique [14] is the simplest one which is to clip the signal below to a predefined threshold, but it is easy for the OFDM system to suffer from serious in-band distortion and the escalation of BER. Although the coding [15], active constellation extension (ACE) [16], [17] and tone reservation (TR) [18], [19] are distortionless techniques, they increase the energy of the transmitted signal. Selected mapping (SLM) technique is on the foundation of the multiple signal representation method, and it has the similar properties as the coding, ACE, and TR. However, the SLM [20] technique is limited in FBMC/OQAM system because of the higher computational complexity. Partial transmit sequences (PTS) [21], [22] is the most widely studied technique of PAPR reduction. By optimizing the PAPR value of each OFDM symbol independently, it is another distortionless method which can effectively reduce PAPR in OFDM system with less computational complexity. Due to the overlapping structure of adjacent data blocks, the conventional PTS technique cannot be employed directly to FBMC/OQAM system. Some PAPR reduction schemes had been proposed for FBMC/OQAM systems based on the conventional PTS technique in OFDM system. In [11], a modified PTS scheme was proposed for the PAPR reduction of the FBMC/OQAM signal by utilizing multi-block joint optimization (MBJO). Although the improved MBJO-PTS scheme could provide a good PAPR reduction result, the complexity would increase by employing a trellis diagram in the MBJO-PTS optimization problem, which made the MBJO-PTS scheme impracticable. A joint optimization scheme was proposed in [12], which combined the linear PTS technique with nonlinear clipping and filtering techniques to effectively reduce the PAPR of FBMC/OQAM signal. However, the effectiveness of reducing the PAPR could had an evident degradation and the computational complexity increase with the increasing number of subblocks.

The PAPR reduction performance of the PTS-based technique mainly depends on the selection of phase factors. The best PAPR reduction performance is offered by the optimal phase factors. However, finding the optimal phase factors is a nondeterministic polynomial-time (NP-hard) problem and the computational complexity of the PTS will increase as the input data number keep increasing. Therefore, the suboptimal solutions are typically preferable. There were some artificial intelligent algorithms methods applied in OFDM system for searching the optimal phase factors in the conventional PTS scheme [23]–[27]. In this paper, we propose a genetic algorithm based bilayer PTS (GA-BPTS) scheme, in which a self-designed prototype filter with low side lobe energy is adopted, to decrease the PAPR of FBMC/OQAM signal and further reduce the computational complexity of the conventional PTS scheme. The main contributions of this paper are listed as follows:

1) In order to have a lower adjacent channel leakage than the OFDM signal, this paper designs a prototype filter to minimize margin side lobe energy.
2) This paper exploits the overlapping structure of the FBMC/OQAM signal. Introducing two penalty operators, the bilayer structure based on the conventional PTS scheme is proposed, and the computational complexity is significantly reduced.
3) To further reduce the search complexity and the PAPR of the traversal algorithm based BPTS (TBPTS) scheme, the GA-BPTS scheme is proposed in the case of large number of the subblocks.
4) The accuracy of the analytical results is demonstrated through numerical simulation. Based on the proposed prototype filter, the proposed GA-BPTS scheme has a remarkable PAPR reduction performance and a lower search complexity than the conventional PTS methods.

The rest of this paper is organized as follows. Section II describes the FBMC/OQAM modulation. In Section III, the GA-BPTS scheme with the self-designed prototype filter is proposed. Section IV presents simulated results for characterizing the proposed PAPR reduction scheme. Finally, conclusions are drawn in Section V.

Notations : we use bold font variables to denote matrices and vectors. $(\cdot)^T$ denotes the transpose, and $\|\cdot\|_2$ denotes the two-norm. $E[\cdot]$ denotes the expectation operator, and $j = \sqrt{-1}$.

II. FBMC/OQAM MODULATION SYSTEM

A. FBMC/OQAM SYSTEM MODEL AND ISI/ICI FORMULA

Fig. 1 illustrates the system model of the FBMC/OQAM system, which consists a transmitter and a receiver [5]. At the transmitter, N subcarriers are composed of the FBMC/OQAM system, and the output of the QAM symbol $S_m = [s_m^0, s_m^1, \cdots, s_m^{N-1}]^T$, $0 \leqslant n \leqslant N-1$, is serial-to-parallel (S/P) converted. The complex input symbols are then written as

$$s_m^n = a_m^n + jb_m^n, \tag{1}$$

where M is the data blocks number. a_m^n and b_m^n are the real and imaginary parts of the m^{th} symbol on the n^{th} subcarrier, respectively. Each symbol's real and imaginary parts are then transmitted on a subcarrier, respectively. For each subcarrier, we use a specially designed prototype filter [28].

The real and imaginary parts are staggered with a $T/2$ time offset, where T is the symbol duration. Fig. 2 shows the FBMC/OQAM symbol structure. After passing through a bank of transmission filters and the phase modulation, the FBMC/OQAM symbols will be treated with the inverse fast fourier transform (IFFT) and polyphase network (PPN).

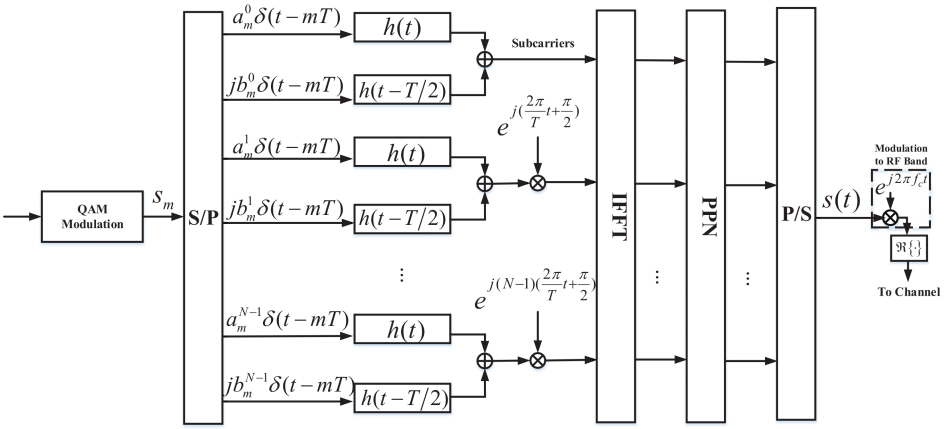

FIGURE 1. A block diagram of FBMC/OQAM transmitter.

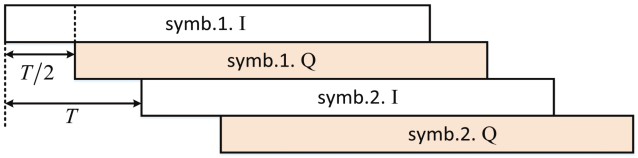

FIGURE 2. The FBMC/OQAM symbol structure.

The modulated FBMC/OQAM signal at sample k is given by (4) shown as

$$s[k] = \sum_{q=-\infty}^{+\infty}\sum_{p=0}^{N-1}(\theta_p a_q^p h[k-qN] + \theta_{p+1} b_q^p h\left[k-qN-\frac{N}{2}\right])e^{jn(k-qN)\frac{2\pi}{N}}, \quad (4)$$

where

$$\theta_p = \begin{cases} 1, & \text{if } p \text{ is even,} \\ j, & \text{if } p \text{ is odd,} \end{cases} \quad (5)$$

and $h[k]$ is the sampled prototype filter. After demodulated from radio frequency (RF) band, the signals are passed to the N matched filters, and the output signals are presented as

$$s_q^p = a_q^p + jb_q^p, \quad (6)$$

where a_q^p and b_q^p represent the real and imaginary parts of the q^{th} received symbol on p^{th} subchannel, respectively.

The $h[k]$ should meet the perfect reconstruction (PR) conditions or to provide nearly perfect reconstruction (NPR) characteristics [28]. However, the PR conditions are only satisfied in an ideal transmission system, which are not indispensable for the prototype filter design. In comparison with the interferences induced by nonideal transmission channels, the interferences caused by the NPR filter are smaller enough than by the PR filter. Moreover, when both of them have the same filter length, the NPR filter is more efficient and can provide lower stop band energy than the PR filter.

We denote the inter-channel interference and inter-symbol interference (ICI/ISI) to a_m^n and b_m^n as $I_{m,n}^a$ and $I_{m,n}^b$, respectively. Then, the expected ISI/ICI interferences power are respectively represented as [28]

$$\begin{aligned}\text{Power}(I_{m,n}^a) &= \mathbb{E}[(a_q^p - a_m^n)^2] \\ &= \mathbb{E}\left[\left(\sum_{q=-\infty}^{\infty}\sum_{p=0}^{N-1} I_{m,n,q,p}^a - a_m^n\right)^2\right], \end{aligned} \quad (7)$$

and

$$\begin{aligned}\text{Power}(I_{m,n}^b) &= \mathbb{E}[(b_q^p - b_m^n)^2] \\ &= \mathbb{E}\left[\left(\sum_{q=-\infty}^{\infty}\sum_{p=0}^{N-1} I_{m,n,q,p}^b - b_m^n\right)^2\right], \end{aligned} \quad (8)$$

where $I_{m,n,q,p}^a$ denotes the contribution of s_q^p to a_q^p and $I_{m,n,q,p}^b$ denotes the contribution of s_q^p to b_q^p. Then we have

$$I_{m,n,q,p}^a = a_q^p C_{m,n,q,p}^1 - b_q^p C_{m,n,q,p}^2, \quad (9)$$

$$a_q^p = \sum_{q=-\infty}^{\infty}\sum_{p=0}^{N-1}\int_{-\infty}^{\infty} h(mT-t)\times\left\{a_q^p\, h(t-qT)\cos[(p-n)\varphi_t] - b_q^p h(t-qT-T/2)\sin[(p-n)\varphi_t]\right\}dt, \quad (2)$$

$$b_q^p = \sum_{q=-\infty}^{\infty}\sum_{p=0}^{N-1}\int_{-\infty}^{\infty} h(mT-t+T/2)\times\left\{a_q^p\, h(t-qT)\sin[(p-n)\varphi_t] - b_q^p h(t-qT-T/2)\cos[(p-n)\varphi_t]\right\}dt. \quad (3)$$

where

$$C^1_{m,n,q,p} = \sum_{k=0}^{L_p-1} \{h[mN-k]h[k-qN] \times \cos[(p-n)(\frac{2\pi k}{TN}+\pi/2)]\}, \quad (10)$$

$$C^2_{m,n,q,p} = \sum_{k=0}^{L_p-1} \{h[mN-k]h[k-qN-\frac{N}{2}] \times \sin[(p-n)(\frac{2\pi k}{TN}+\pi/2)]\}. \quad (11)$$

Attributable to the randomness of information bits, a^n_m, a^p_q, b^n_m, and b^p_q are assumed as Gaussian random variables that are statistically independent and identically distributed (i.i.d.).

$$\mathbb{E}\left[(a^p_q)^2\right] = \mathbb{E}\left[(b^p_q)^2\right] = 1, \quad (12)$$

$$\mathbb{E}\left[a^p_q\right] = \mathbb{E}\left[b^p_q\right] = 0. \quad (13)$$

From (7), (12) and (13), we can obtain

$$\mathbb{E}\left[(I^a_{m,n,q,p})^2\right] = (C^1_{m,n,q,p})^2 + (C^2_{m,n,q,p})^2. \quad (14)$$

If $(m, n) = (q, p)$, we have

$$C^1_{m,n,q,p} = \sum_{k=0}^{L_p-1} h[k]^2, \quad (15)$$

$$C^2_{m,n,q,p} = 0. \quad (16)$$

Therefore,

$$I^a_{m,n,q,p} = a^n_m \sum_{k=0}^{L_p-1} h[k]^2. \quad (17)$$

Apparently, it should be satisfied that

$$\sum_{k=0}^{L_p-1} h[k]^2 = 1, \quad (18)$$

$$I^a_{m,n,q,p} = a^n_m. \quad (19)$$

Otherwise, we have

$$\text{Power}(I^a_{m,n}) = \sum_{q=-\infty}^{\infty} \left\{ \sum_{p=0,(q,p)\neq(m,n)}^{N-1} \mathbb{E}\left[\left(I^a_{m,n,q,p}\right)^2\right] \right\}. \quad (20)$$

Given that all the symbols are independent and identically distributed (i.i.d.), Power($I^a_{m,n}$) and Power($I^b_{m,n}$) are independent of m, n, and then we can use any choice of m, n to measure the ISI/ICI of the entire system. Without loss of generality, we set $q = p = 0$. Under normal circumstances, the ISI/ICI caused from adjacent subcarriers and adjacent symbols are larger than that of non-adjacent subcarriers and non-adjacent symbols. In order to simplify the calculation, we set $-1 \le m \le 1$, $-1 \le n \le 1$ [28].

B. PROTOTYPE FILTER DESIGN SCHEME

Due to the advantageous properties of the prototype filter, the FBMC/OQAM signal will have a better adjacent channel leakage ratio than the OFDM signal [10]. We formulate the filter coefficients related direct optimization problem before the processing of PAPR reduction. In order to mitigate the effects between adjacent subchannels, the transition between subchannels should located at the center among adjacent subcarriers when $\omega = \frac{2\pi}{N}$. Moreover, we choose the criterion of minimum stop band energy to design the prototype filter for FBMC/OQAM system. The threshold TH is introduced to limit the ISI/ICI energy within a certain range and then the BER of the transmitted and received signals can be controlled to satisfy the NPR property. On the foundation of the relationship that Power($I^a_{m,n}$) = Power($I^b_{m,n}$), we only consider the ISI/ICI of real part in our optimization problem in the following analysis.

The filter $h[k]$ with length L_p is chosen, whose coefficients are constrained to be real and even to automatically satisfy the NPR characteristics [29], i.e.,

$$h[k] = h\left[L_p - 1 - k\right], \quad k = 0, 1, \ldots, L_p - 1. \quad (21)$$

The fourier transform of the $h[k]$ is

$$H\left(e^{j\omega}\right) = \sum_{k=0}^{L_p-1} h[k]\, e^{-j\omega k}. \quad (22)$$

Then, the magnitude response of the $h[k]$ is

$$\left|H\left(e^{j\omega}\right)\right| = \left|\sum_{k=0}^{L_p-1} h[k]\, e^{-j\omega k}\right|. \quad (23)$$

In order to achieve the suppression of side lobe energy and reduce the side lobe leakage, we divide the stop band region into three segments, where the stop band region is denoted as $[\frac{2\pi}{N}, \pi]$. Let P_1, P_2, P_3 denote the energy of each segment, and they are given as

$$P_1 = \int_{\omega_0}^{2\omega_0} \left|H(e^{j\omega})\right|^2 d\omega,$$

$$P_2 = \int_{2\omega_0}^{3\omega_0} \left|H(e^{j\omega})\right|^2 d\omega,$$

$$P_3 = \int_{3\omega_0}^{\pi} \left|H(e^{j\omega})\right|^2 d\omega. \quad (24)$$

With P_1 and the total stop band energy constrained to the predefined threshold, let the equation (36), (21) be satisfied, and limit the ISI/ICI energy to a needed level, then we minimize the P_2 and P_3. The optimization problem **P1** is formulated as

$$\mathbf{P1}: \min_{\boldsymbol{h}} P_2(\boldsymbol{h}) + P_3(\boldsymbol{h}), \quad (25a)$$

$$\text{s.t. } h[k] = h\left[L_p - 1 - k\right], \quad (25b)$$

$$\text{Power}(I^a_{m,n}) < TH, \quad (25c)$$

$$\text{Power}(I^b_{m,n}) < TH, \quad (25d)$$

$$\sum_{k=0}^{L_p-1} h[k]^2 = 1, \tag{25e}$$

$$P_1(\boldsymbol{h}) \le Q_1, \tag{25f}$$

$$P(\boldsymbol{h}) \le Q \tag{25g}$$

where $\boldsymbol{h} = [h[0], h[k], \cdots, h[L_p - 1]]^T$, $P = \sum_{i=1}^{3} P_i(\boldsymbol{h})$ is the total stop band energy, and Q_1, Q are the predefined levels for the P_1 and P respectively.

Three different optimal objective functions P_2, P_3, and $P_2 + P_3$ can be chosen to optimize the constraint factor for oriented side lobe energy suppression. Due to the similar mathematical formulations between P_2 and P_3, for simplicity, we choose P_3 and $P_2 + P_3$ as the optimal objective functions in this paper. After analyzing the above optimization problem **P1**, we know that **P1** is a nonlinear and nonconvex optimization problem. The sequential quadratic programming (SQP) algorithm [30] is considered as an effective method to solve the optimization problem.

III. THE PEAK-TO-AVERAGE POWER RATIO (PAPR) IN FBMC/OQAM SYSTEM

After obtaining the well-designed prototype filter with small enough side lobe energy leakage, we aim to reduce the PAPR of the FBMC/OQAM signal. In practice, it is hard to straightforwardly measure the PAPR of the continuous-time signal in the baseband, so most of the existing schemes of PAPR reduction are applied in the discrete-time signal. However, the PAPR implemented in the discrete-time baseband signal $s[k]$ may be different with that in the continuous-time baseband signal. The $s(t)$ is β-times oversampled to approach the true PAPR of the FBMC/OQAM signal to a maximum extent, where $\beta \geqslant 4$ [13].

Taking the overlapping structure of FBMC/OQAM signals into consideration, we define a frame which contains M overlapping FBMC/OQAM data blocks. If the length of each FBMC/OQAM block is $\left(\beta + \frac{1}{2}\right)N$, $\left(M + \beta - \frac{1}{2}\right)N$ will be the length of the frame. Therefore, the PAPR value of a FBMC/OQAM frame can be represented with $s[k]$ in dB as [17]

$$\mathrm{PAPR}(s_f)_{\mathrm{dB}} = 10\log_{10}\left(\frac{\max\limits_{0\leqslant k\leqslant\left(M+\beta-\frac{1}{2}\right)N-1} \left|\{s_f\}_k\right|^2}{E\left[\left|s_f\right|^2\right]}\right). \tag{26}$$

where $s_f = \left[s[0], \cdots, s\left[\left(M + \beta - \frac{1}{2}\right)N - 1\right]\right]^T$.

A. CONVENTIONAL PTS SCHEME

In OFDM system, the conventional PTS technique partitions the input data block S into V disjoint subblocks S^v, $v = 1, 2, \cdots, V$. The discrete-time domain signal then be denoted as

$$S = \left[S^0, S^1, \cdots, S^v, \cdots, S^V\right]^T, \tag{27}$$

where each component S^v is with equal length and located consecutively at S.

Then, the phase factors are employed to independently rotate the subcarriers of each subblock, which can result in the envelope fluctuations of OFDM signals. In general, traversal searching algorithm is applied for appropriate combination of each subblock and its multiplied phase factors to minimize the PAPR, and therefore the optimal phase factors can be obtained. The set of the phase factors are denoted as a vector, i.e. $b = \left\{b^v = e^{j2\pi l/W} \middle| l = 0, 1, \cdots, W-1\right\}$ where W is the number of allowable phase factors. In order to reduce the search complexity, there is a limitation imposed on the selection of phase factors that the number of allowable phase factors is set to finite number.

The overlapping structure of FBMC/OQAM signals is shown in Fig. 2, it is clear to conclude that the m^{th} block overlaps with the next $\beta - 1$ data blocks. Employing the conventional PTS technique for the FBMC/OQAM system, block S_m should be partitioned into V subblocks. The discrete-time domain sequences of the v^{th} subblock is represented with $s_m^v[k]$, and $s_m^v[k]$ is denoted as

$$s_m^v[k] = \left(s_m^{v,0}[k], s_m^{v,1}[k], \cdots, s_m^{v,n}[k], \cdots, s_m^{v,N-1}[k]\right), \tag{28}$$

where $s_m^{v,n}[k] = s_m^n[k]$, if n^{th} symbol belongs to subblock v.

The signal of the v^{th} subblock is given by

$$s_m^v[k] = \sum_{n=0}^{N-1} s_m^{v,n}[k], \tag{29}$$

Therefore, the m^{th} data block with phase factor vector b_m^v is

$$s_m[k] = \sum_{v=1}^{V} b_m^v s_m^v[k]. \tag{30}$$

PAPR can be minimized by selecting the optimal phase factors vector, which is given by

$$\left[\tilde{b}_m^1, \cdots, \tilde{b}_m^V\right] = \arg \min_{\left[b_m^1, \cdots, b_m^V\right]} \left(\max_{(m-1)N\leqslant k\leqslant(\beta+m-\frac{1}{2})N-1} \left|\sum_{v=1}^{V} b_m^v s_m^v[k]\right|\right), \tag{31}$$

Thus, the discrete-time domain signal that has the lowest PAPR value is represented as [18]:

$$\tilde{s}_m[k] = \sum_{v=1}^{V} \tilde{b}_m^v s_m^v[k]. \tag{32}$$

However, the phase rotation operation is only applied for the present data block in the conventional PTS scheme. As shown in Fig.2, for the overlapping nature of FBMC/OQAM signals, the direct application of conventional PTS technique into the FBMC/OQAM system will greatly debase the optimization performance.

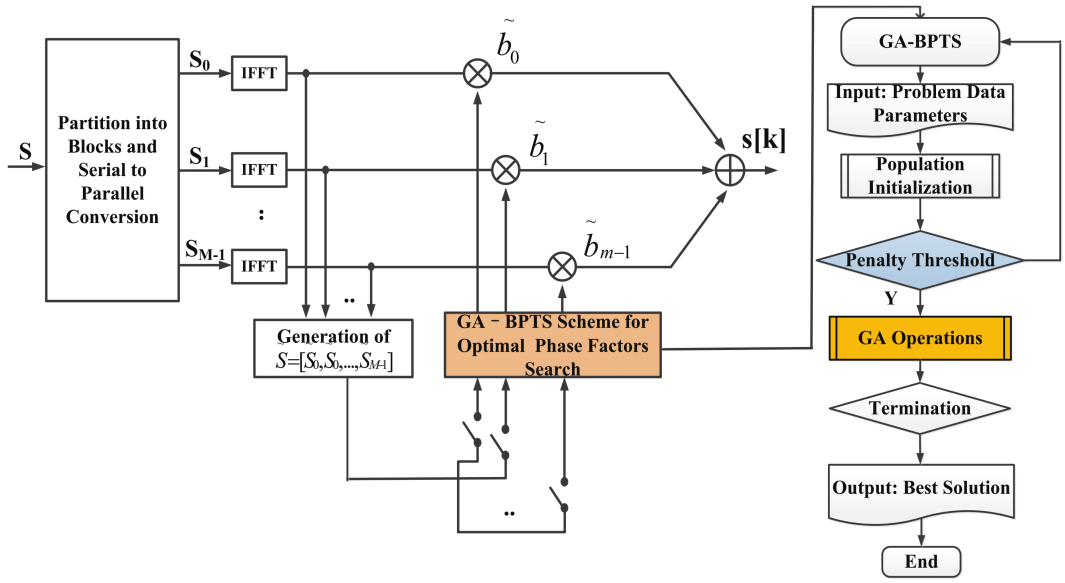

FIGURE 3. Block diagram of the GA-BPTS scheme.

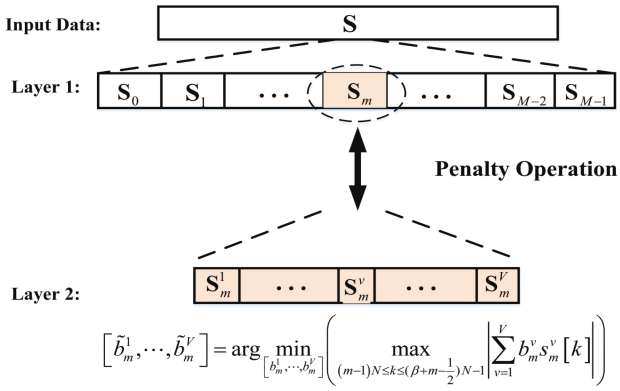

FIGURE 4. Structure of the bilayer PTS scheme.

B. GA-BASED BPTS SCHEME

For the PAPR reduction of FBMC/OQAM signal, we propose the GA-based BPTS scheme. The block diagram of GA-BPTS scheme is shown in Fig. 3. This scheme exploits the overlapping structure of FBMC/OQAM signal, and is adequate for PAPR minimization in the FBMC/OQAM signal with 4 up-sampling. With the help of the above proposed prototype filter, the scheme aims to reduce search complexity of the conventional PTS scheme, but is not at the cost of system performance.

1) TBPTS SCHEME WITH PENALTY OPERATORS

As shown in Fig. 4, the data block S_m containing M overlapping FBMC/OQAM data is divided into V subblocks by using the adjacent partition method, and $0 \leqslant m \leqslant M-1$, that is

$$S_m = \sum_{v=1}^{V} S_m^v, \tag{33}$$

Combining the candidate vector of phase factors $b_m = \left[\tilde{b}_m^1, \cdots, \tilde{b}_m^v, \cdots, \tilde{b}_m^V\right]$ with the corresponding V subblocks in the layer 2, the PAPR minimization problem of the FBMC/OQAM signal is then written as **P2**.

$$\mathbf{P2}: \min_{b_m} \left\{ \max_k |\tilde{s}_m[k]|^2 \right\} \tag{34a}$$

$$\text{s.t. } \tilde{s}_m[k] = \sum_{v=1}^{V} \tilde{b}_m^v s_m^v[k] \tag{34b}$$

$$b_m^v = \left\{ e^{j2\pi l/W} \middle| \, l = 0, 1, \cdots, W-1 \right\} \tag{34c}$$

$$1 \leqslant v \leqslant V \tag{34d}$$

$$0 \leqslant n \leqslant N-1 \tag{34e}$$

The computational complexity of the minimization problem **P2** consists of three parts [21]:

i) The value of overlapping factor β;
ii) The phase factors $\tilde{b}_m$ and the number of data blocks M and V;
iii) The PAPR computation.

For part i), we have chosen the overlapping factor $\beta = 4$ to mitigate the overlapping effects, and to close to the true PAPR of the continous-time signal very well. So the main consideration for computational complexity reduction is focused on part ii) and part iii).

Firstly, the phase factors $\tilde{b}_m$ are only chosen from $\{-1, 1\}$ with $W = 2$ for all v and m; Secondly, two ***penalty operators*** μ_p and ω_p are introduced to find the suboptimal solution b_m^* in **P2**. Different from the conventional clipping technique in which the penalty factors will lead to the distortion of FBMC/OQAM signals, the ***penalty operators*** will not result in distortion.

Let

$$\mu_p = \frac{1}{\sqrt{2}} \max_k \{|s[k]|\}, \tag{35}$$

Algorithm 1 Traversal Algorithm Based BPTS Phase Factors Search

Initialize $\tilde{b}_m = [1, 1, \cdots, 1]$ and $index = 1$, compute the PAPR of the $\tilde{b}_m$ combined signal, named PAPR_0;
while $index < V + 1$ **do**
  $\tilde{b}_m[index] = -1$;
  Recompute the PAPR, named PAPR_{index};
  if $\text{PAPR}_{index} \leqslant \text{PAPR}_0$ **then**
    Retain $\tilde{b}_m[index]$ as part of the final set of phase factors;
  else
    $\tilde{b}_m[index] = 1$;
  end if
  $index = index + 1$;
end while

The penalty operators μ_p and ω_p are set to ***punish*** the data blocks that meet either of the following two conditions, and then to execute the **Algorithm 1**; otherwise, there is no action performing on the subblock S_m^v. The ***punish*** conditions are

$$1)\xi \geqslant \omega_p; \quad 2)\max_k \left\{|s_m[k]|^2\right\} \geqslant \frac{1}{\sqrt{2}} \max_k \left\{|s[k]|^2\right\} \tag{36}$$

where

$$\xi = \text{num}\left(|s_m[k]| \geqslant \mu_p \left| (m-1)N \leqslant k \leqslant (\beta + m - \frac{1}{2})N - 1\right.\right) \tag{37}$$

To sum up, the proposed TBPTS scheme with penalty operators is shown in **Algorithm 1**.

2) GA BASED BPTS PHASE FACTORS SEARCH SCHEME

Introduced by Holland [23] and drawn on the experience of the biological evolution principle in nature, GA is a common function optimization method, which has the globally searching capability to obtain the best or a better approximation solution with the help of the bio-inspired operators, known as selection, crossover and mutation [31], [32], [37].

- **Encoding:** For each individual in GA, the most widely used encoding methods [33] is that establishing a binary vector with constant length. In the population $\mathcal{N}$, a certain number of encoded individuals represent the candidate solutions of the optimization problem **P2**. Especially, we give the coding rule when $W = 2, V = 32$ to the proposed GA-BPTS scheme. In this case, $\tilde{b}_m^v \in b = (b_0, b_1) = (1, -1)$ and $log_2\, W$ bit binary encoding is applied for each phase factors. Moreover, we define that binary code "**1**" represents phase factor $b_0 = 1$ and binary code "**0**" represents phase factor $b_1 = -1$. Therefore, the individual $b_m = \left[\tilde{b}_m^1, \cdots, \tilde{b}_m^v, \cdots, \tilde{b}_m^V\right]$ is encoded into a 32-bit binary vector. The entire encoded population $\mathcal{N}$ can be denoted as

$$\mathcal{N} = [\theta_1, \cdots, \theta_i, \cdots, \theta_P], \tag{38}$$

Algorithm 2 Genetic Algorithm Based BPTS Phase Factors Search

Input: Maximal Number of Iterations Q, $s_m^v[k]$ of the m^{th} candidate data block $s_m[k]$;
Output: Optimal phase factors b_m^* of the m^{th} candidate data block $s_m[k]$;
Initialize the population $\mathcal{N}_0$ of size P;
$index \leftarrow 0$, get fitness f_0 of Population $\mathcal{N}_0$;
while $index < Q$ **do**
  Crossover parent individuals with adaptive probabilities P_c to generate new candidate offspring b_m^{Cro};
  Calculate fitness f_c of b_m^{Cro} based on Equation (39);
  Mutate parent individuals with adaptive probabilities P_m to generate new candidate offspring b_m^{Mut};
  Calculate fitness f_m of b_m^{Mut} based on Equation (39);
  if $\left|f_{index}^* - f_{index-1}^*\right| \leq \Delta f$ **then**
    $CountBreak++$;
    $f_{index-1}^* = f_{index}^*$;
  else
    $CountBreak = 0$;
  end if
  if $CountBreak \geq N$ **then**
    Break;
  end if
  Find out the maximal fitness f_{index}^* among f_{index}, f_c, and f_m based on Equation (40);
  Mark the the b_m^{max} value that corresponds to f_{index}^*.
  Elitist Selection combined with *Roulette Wheel Selection* to get next population $\mathcal{N}_{index+1}$;
  $index \leftarrow index + 1$;
end while
$b_m^* = b_m^{max}$;
return b_m^*

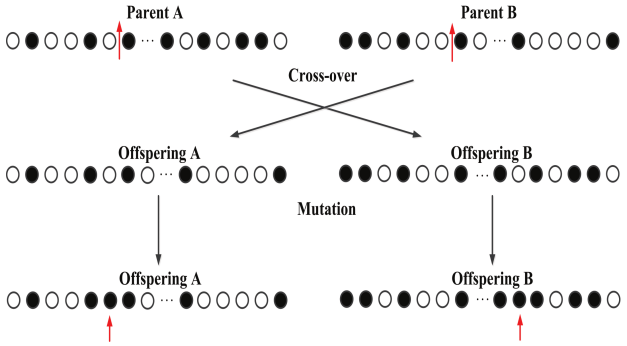

FIGURE 5. Genetic Operations.

where θ_i is the 32-bit encoded vector of each GA-BPTS individual, and P is the number of population $\mathcal{N}$.

- **Fitness Evaluation Function:** Let fitness f_i represent each individual's adaptability in $\mathcal{N}$ [34]. In this paper, the formula to calculate the GA-BPTS individuals' *fitness* in $\mathcal{N}$ is given by

$$f_i(\tilde{s}_m[k]) = \frac{1}{10log_{10}PAPR(\tilde{s}_m[k])}, \tag{39}$$

In addition, the maximal fitness of all the individuals in $\mathcal{N}$ is given by

$$f^* = \max_{1\le i\le P} f_i, \tag{40}$$

- **Mutation and Crossover Operation:** The operations of crossover and mutation play an important role in the GA, and therefore suitable operations are needed to pass good genes to the offspring. In the traditional GA, the probability P_c and P_m are applied to control the evolutionary processes of the crossover and mutation operators. However, the fixed probability of P_c and P_m may result in poor performance of convergence speed and the quality of solution. In order to improve the optimization ability of the GA-BPTS scheme, the adaptive genetic operators [34] are applied to escape from the local optimum. The expressions are given as

$$P_c = \begin{cases} P_{c1} - \dfrac{(P_{c1}-P_{c2})(f-f_{\text{avg}})}{f_{\max}-f_{\text{avg}}}, & f > f_{\text{avg}} \\ P_{c1}, & f < f_{\text{avg}} \end{cases}$$
$$P_m = \begin{cases} P_{m1} - \dfrac{(P_{m1}-P_{m2})(f-f_{\text{avg}})}{f_{\max}-f_{\text{avg}}}, & f > f_{\text{avg}} \\ P_{m1}, & f < f_{\text{avg}} \end{cases} \tag{41}$$

  where P_{c1} and P_{c2} are the upper and lower bounds of crossover probability, respectively. P_{m1} and P_{m2} are the upper and lower bounds of mutation probability, respectively. $f_{\max}$ and f_{avg} are the maximal fitness value and average fitness value of individuals in a population, respectively.

  An illustration of the crossover and mutation operations is depicted in Fig 5, let black balls represent binary code "**1**" and white balls represent binary code "**0**". A 32-bit binary vector Λ_r is randomly generated, and the positions of binary code "**1**" of Λ_r are recorded as a set Λ_r^1. Genes whose positions correspond to the points in the set Λ_r^1 are selected to separated from the two parents, and crossed-over by the adaptive genetic probability P_c to generate new descendants. The similar process can be adopted for the mutation.
- **Selection Operation:** In order to prevent good features of the current population from being discarded in the next generation, the *elitist selection* [35] is combined with *roulette wheel selection* [36] in our selection process. Based on the fitness values of all of individuals which include parents and their crossover-mutated descendants, these individuals are arranged in descending order. Then the top S most-fit individuals (i.e., Elitists) are passed directly into the next generation, while the $P-S$ individuals are chosen by the *roulette wheel selection*. Thus, the next new population is constructed with the constant size P.
- **Termination Criterion:** The iteration will be terminated once either the maximal fitness value maintains stable in successive N generations or the maximal iteration number Q is reached. The pseudocode of the proposed GA-BPTS scheme is summarized in **Algorithm 2**.

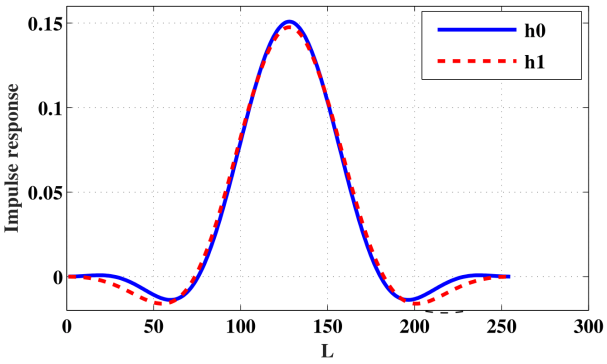

FIGURE 6. Impulse response of the filters $h0$ and $h1$.

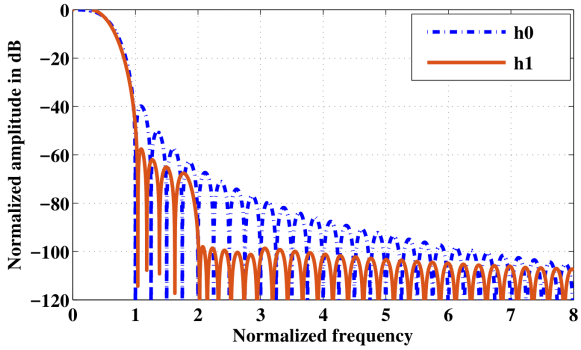

FIGURE 7. Normalized magnitude responses of the filters $h0$ and $h1$.

IV. NUMERICAL RESULTS

In this section, simulation results are conducted to investigate the PAPR reduction performance of the proposed GA-BPTS scheme. The number of the subcarriers N is set to 128 and 4 QAM modulation is adopted for the FBMC/OQAM system. $Q_1 = -70$dB, $Q = -75$dB, and $TH = 10^{-4}$ are set for optimization **P1**, and $\omega_p = 2$. FBMC/OQAM signal requires a prototype filter with long length to achieve good performance, but it is hard for practical implementation and is inferior in the future burst communication. Without special emphasis, $L = 256$ is considered for the following simulation.

Fig. 6 shows the impulse responses of the start-of-the-art PHYDAYS [9] filter $h_0[k]$ and the proposed filter $h_1[k]$. As we all know, PHYDAYS filter is the most widely used prototype filter with NPR property in FBMC/OQAM system. Compared with the filter $h_0[k]$, there is a noticeable improvement in stop band energy suppression of the proposed filter $h_1[k]$, which means that the $h_1[k]$ can effectively reduce the out-of-band energy leaks.

Fig. 7 illustrates the normalized magnitude responses of the PHYDAYS filter $h_0[k]$ and the proposed filter $h_1[k]$. It is observed that the overall stop band energy of $h_1[k]$ are -76dB, which are significantly lower than the value of the $h_0[k]$, -63dB by about 13dB. In addition, the proposed filter $h_1[k]$ aiming to minimize the margin side lobe energy

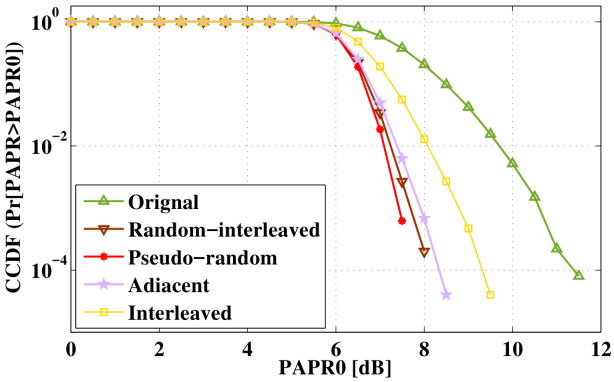

FIGURE 8. Different partition methods.

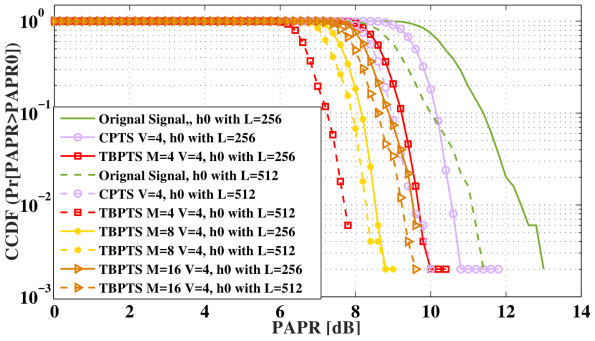

FIGURE 10. The PAPR reduction results of the TBPTS scheme with different subblocks, prototype filter length *L*.

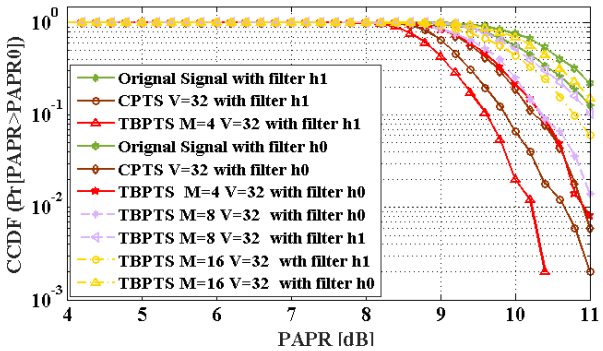

FIGURE 9. The PAPR reduction results of the TBPTS scheme with different prototype filter, $V = 32$.

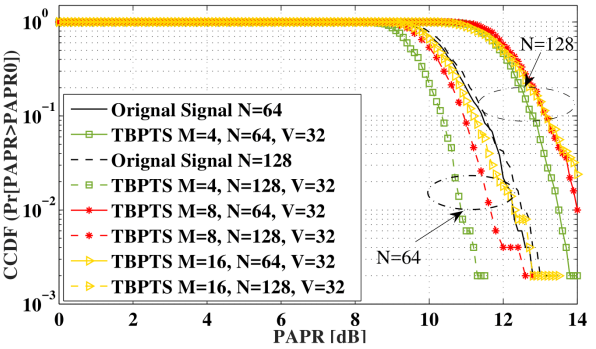

FIGURE 11. The PAPR reduction results of the TBPTS scheme with different subcarriers *N*, proposed prototype filter *h*1, $V = 32$.

(i.e.$P_2 + P_3$) has the better side lobe energy suppression performance than that of the PHYDAYS filter $h_0[k]$. These simulation results verify that the prototype filter $h_1[k]$ obtained by the proposed optimization model $P1$ has the better performance of out-of-band attenuation than the PHYDAYS filter $h_0[k]$ in FBMC/OQAM system and the proposed scheme achieves the oriented side lobe energy suppression in FBMC.

In the conventional PTS technique, the subblock partition methods can be classified into three categories: pseudo-random partition, interleaved partition and adjacent partition [12]. Fig. 8 displays the complementary cumulative distribution function (CCDF) comparison of different PTS partition methods with $M = 4$ in the FBMC/OQAM system. The PAPR reduction performance achieved by pseudo-random partition method is obviously more superior to the other two methods. However, the pseudo-random partition method is usually uncertain and variable, which may make the system performance lack of stability or acceptability. Therefore, based on the simulation results of Fig. 8, we choose the adjacent partition method in this paper.

In order to better reveal the effect of the prototype filter on PAPR reduction for FBMC/OQAM signal, Fig. 9 plots the PAPR reduction results with different prototype filters $h[k]$ for pretreatment before TBPTS scheme and $V = 32$. It shows us the proposed filter $h_1[k]$ outperforms the PHYDAYS filter $h_0[k]$ in PAPR reduction of the FBMC/OQAM signal. In addition, when the subblocks change from $V = 4$ to $V = 32$, compared with the CPTS scheme, the TBPTS has a poor PAPR reduction performance except for $M = 4$, $V = 32$ with filter $h_1[k]$. Then, we can conclude that the effectiveness of reducing the PAPR also can have an evident degradation with the increasing number of subblocks V in layer 2.

Fig. 10 shows the PAPR reduction results of the TBPTS scheme with different subblocks M in layer 1, and prototype filter $h_0[k]$ with length $L = 256$ and $L = 512$ are adopted before the TBPTS processing, respectively. Compared with the conventional PTS (CPTS) scheme under the same filter length L, the TBPTS scheme with different subblock M can effectively reduce the PAPR of the FBMC/OQAM signal, which confirms the validity of the TBPTS scheme. Moreover, under the same subblock M, we can see that the longer the filter length, the better PAPR reduction performance of the TBPTS. However, as the number of M increases, the performance of the TBPTS scheme has a degradation, especially, when the $M = 16$, $L = 256$, TBPTS scheme has a similar performance of reducing the PAPR with CPTS scheme.

Fig. 11 plots the PAPR reduction results with varying subcarriers number N, and the proposed prototype filters $h_1[k]$ is adopted for pretreatment before TBPTS scheme. The CCDF results for two numbers of subcarriers $N = 64$ and $N = 128$ are shown, which shows us that with the subcarriers numbers increasing, the PAPR reduction performance deteriorates. The result is consistent with the inherent properties of the multi-carrier system.

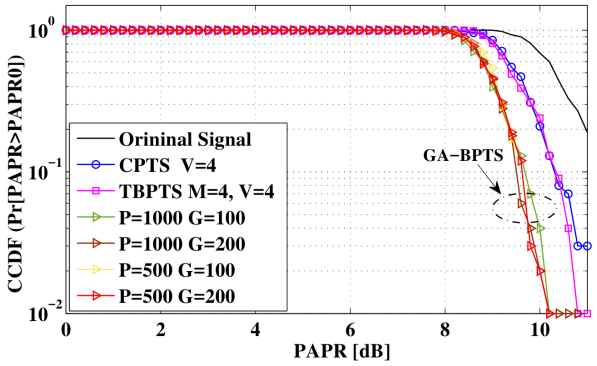

FIGURE 12. The PAPR reduction results of the GA-BPTS scheme, proposed prototype filter $h1$, $V = 32$.

TABLE 1. Computational complexity and the real computing time.

Schemes	Computational Complexity	Computing Time
CPTS	$\mathcal{O}\left(W^{M-1}\right)$	63.4s
TBPTS	$\mathcal{O}\left(MW^{V-1}\right)$	306.3s
GA-BPTS (P=1000, G=100)	$\mathcal{O}\left(M(P*Q)\right)$	205.7s
GA-BPTS (P=1000, G=200)	$\mathcal{O}\left(M(P*Q)\right)$	206.7s
GA-BPTS (P=500, G=100)	$\mathcal{O}\left(M(P*Q)\right)$	106.1s
GA-BPTS (P=500, G=200)	$\mathcal{O}\left(M(P*Q)\right)$	105s

In Fig. 12, we show the CCDF curves after the GA-BPTS scheme processing with varying population and generation size, and the proposed filter $h_1[k]$ is used for pretreatment. As can be observed, with the population and generation size increasing, the PAPR could be reduced by using the GA-BPTS scheme. Especially, compared with the best solution of the TBPTS scheme in $M = 4, V = 4$ and the CPTS scheme when $CCDF = 10^{-2}$, the PAPR values are all close to 10dB, lower than the PAPR values obtained by the other two schemes.

The computational complexity and the real computing time of the CPTS scheme, TBPTS scheme, and GA-BPTS scheme are showed in Table 1, and the simulation parameters are the same as Fig. 12. Combined with Fig. 12, it is observed that the computational complexity of the GA-BPTS scheme is $\mathcal{O}\left(M(P*Q)\right)$ and the real computing time of the GA-BPTS is 206.7s in the worst case, and the real computing time of the traditional PTS algorithm has a little advantage when the number of subblocks is relatively small, but the PAPR reduction performance is very poor. Therefore, the GA-BPTS scheme outperforms the TBPTS scheme and the CPTS scheme in terms of the PAPR reduction with lower computational complexity. What is worth mentioning is that the GA-BPTS scheme could obtain a better PAPR reduction results when the maximum population and generation size increase, but the computational complexity will increase at the same time, and we should choose the appropriate population and generation size of the GA-BPTS scheme to keep the better PAPR reduction performance and decrease the computational complexity.

V. CONCLUSION

In this paper, an GA-BPTS scheme has been proposed for the PAPR reduction of the FBMC/OQAM system. Using the GA algorithm to search the suboptimal phase factors in the bilayer PTS structure, and with the help of a advantageous prototype filter, the PAPR reduction performance of the FBMC/OQAM system has a remarkable improvement. Conducted simulation results show that an FBMC/OQAM system with the GA-BPTS scheme is able to achieve better PAPR reduction than the other conventional schemes and significantly reduce the computational complexity.

REFERENCES

[1] P. Banelli, S. Buzzi, G. Colavolpe, A. Modenini, F. Rusek, and A. Ugolini, "Modulation formats and waveforms for 5G networks: Who will be the heir of OFDM?: An overview of alternative modulation schemes for improved spectral efficiency," *IEEE Signal Process. Mag.*, vol. 31, no. 6, pp. 80–93, Nov. 2014.

[2] S. Ni, J. Zhao, H. H. Yang, and Y. Gong, "Enhancing downlink transmission in MIMO HetNet with wireless backhaul," *IEEE Trans. Veh. Technol.*, vol. 68, no. 7, pp. 6817–6832, Jul. 2019.

[3] J. Zhao, S. Ni, L. Yang, Z. Zhang, Y. Gong, and X. You, "Multiband cooperation for 5G HetNets: A promising network paradigm," *IEEE Veh. Technol. Mag.*, vol. 14, no. 4, pp. 85–93, Dec. 2019.

[4] B. Farhang-Boroujeny, "OFDM versus filter bank multicarrier," *IEEE Signal Process. Mag.*, vol. 28, no. 3, pp. 92–112, May 2011.

[5] M. Bellanger, "Physical layer for future broadband radio systems," in *Proc. IEEE Radio Wireless Symp. (RWS)*, New Orleans, LA, USA, Jan. 2010, pp. 436–439.

[6] J. Nadal, C. A. Nour, and A. Baghdadi, "Design and evaluation of a novel short prototype filter for FBMC/OQAM modulation," *IEEE Access*, vol. 6, pp. 19610–19625, 2018.

[7] D. Qu, F. Wang, Y. Wang, T. Jiang, and B. Farhang-Boroujeny, "Improving spectral efficiency of FBMC-OQAM through virtual symbols," *IEEE Trans. Wireless Commun.*, vol. 16, no. 7, pp. 4204–4215, Jul. 2017.

[8] Z. Junhui, Y. Tao, G. Yi, W. Jiao, and F. Lei, "Power control algorithm of cognitive radio based on non-cooperative game theory," *China Commun.*, vol. 10, no. 11, pp. 143–154, Nov. 2013.

[9] J. Kim, Y. Park, S. Weon, J. Jeong, S. Choi, and D. Hong, "A new filter-bank multicarrier system: The linearly processed FBMC system," *IEEE Trans. Wireless Commun.*, vol. 17, no. 7, pp. 4888–4898, Jul. 2018.

[10] M. Bellanger, D. Le Ruyet, D. Roviras, M. Terré, J. Nossek, L. Baltar, Q. Bai, D. Waldhauser, M. Renfors, T. Ihalainen, and A. Viholainen, "FBMC physical layer: A primer," *PHYDYAS*, vol. 25, no. 4, pp. 7–10, Jan. 2010.

[11] D. Qu, S. Lu, and T. Jiang, "Multi-block joint optimization for the peak-to-average power ratio reduction of FBMC-OQAM signals," *IEEE Trans. Signal Process.*, vol. 61, no. 7, pp. 1605–1613, Apr. 2013.

[12] J. Zhao, S. Ni, and Y. Gong, "Peak-to-average power ratio reduction of FBMC/OQAM signal using a joint optimization scheme," *IEEE Access*, vol. 5, pp. 15810–15819, 2017.

[13] T. Jiang and Y. Wu, "An overview: Peak-to-average power ratio reduction techniques for OFDM signals," *IEEE Trans. Broadcast.*, vol. 54, no. 2, pp. 257–268, Jun. 2008.

[14] M. U. Rahim, T. H. Stitz, and M. Renfors, "Analysis of clipping-based PAPR-reduction in multicarrier systems," in *Proc. IEEE Veh. Tech. Conf. (VTC) Spring*, Barcelona, Spain, Apr. 2009, pp. 1–5.

[15] A. Jones, T. Wilkinson, and S. Barton, "Block coding scheme for reduction of peak to mean envelope power ratio of multicarrier transmission schemes," *Electron. Lett.*, vol. 30, no. 25, pp. 2098–2099, Dec. 1994.

[16] Z. Yang, H. Fang, and C. Pan, "ACE with frame interleaving scheme to reduce peak-to-average power ratio in OFDM systems," *IEEE Trans. Broadcast.*, vol. 51, no. 4, pp. 571–575, Dec. 2005.
[17] D. N. N. Van, B. T. Maharaj, L. F. De, G. J. González, F. Gregorio, and J. Cousseau, "PAPR reduction in FBMC using an ACE-based linear programming optimization," *EURASIP J. Adv. Signal Process.*, vol. 2014, no. 1, p. 172, 2014.
[18] H. Wang, X. Wang, L. Xu, and W. Du, "Hybrid PAPR reduction scheme for FBMC/OQAM systems based on multi data block PTS and TR methods," *IEEE Access*, vol. 4, pp. 4761–4768, 2016.
[19] S. Lu, D. Qu, and Y. He, "Sliding window tone reservation technique for the peak-to-average power ratio reduction of FBMC-OQAM signals," *IEEE Wireless Commun. Lett.*, vol. 1, no. 4, pp. 268–271, Aug. 2012.
[20] D.-W. Lim, J.-S. No, C.-W. Lim, and H. Chung, "A new SLM OFDM scheme with low complexity for PAPR reduction," *IEEE Signal Process. Lett.*, vol. 12, no. 2, pp. 93–96, Feb. 2005.
[21] Y. Xiao, X. Lei, Q. Wen, and S. Li, "A class of low complexity PTS techniques for PAPR reduction in OFDM systems," *IEEE Signal Process. Lett.*, vol. 14, no. 10, pp. 680–683, Oct. 2007.
[22] J. Hou, J. Ge, and J. Li, "Peak-to-average power ratio reduction of OFDM signals using PTS scheme with low computational complexity," *IEEE Trans. Broadcast.*, vol. 57, no. 1, pp. 143–148, Mar. 2011.
[23] E. A. A. Hagras, S. A. Fathy, and M. S. El-Mahallawy, "Genetic algorithm based tone-reservation for PAPR reduction in wavelet-OFDM systems," in *Proc. 33rd Nat. Radio Sci. Conf. (NRSC)*, Aswan, Egypt, Feb. 2016, pp. 223–232.
[24] J. Shukla, A. Joshi, R. Bansal, and R. Tyagi, "PAPR reduction of OFDM systems using PTS with genetic algorithm at low computational complexity," in *Proc. Int. Conf. Recent Adv. Innov. Eng. (ICRAIE)*, Jaipur, India, May 2014, pp. 1–6.
[25] X. Cheng, D. Liu, S. Feng, H. Fang, and D. Liu, "An artificial bee colony-based SLM scheme for PAPR reduction in OFDM systems," in *Proc. 2nd IEEE Int. Conf. Comput. Intell. Appl. (ICCIA)*, Wuhan, China, Sep. 2017, pp. 449–453.
[26] P. Kaur and M. Singh, "Performance analysis of GA-PTS for PAPR reduction in OFDM system," in *Proc. Int. Conf. Wireless Commun., Signal Process. Netw. (WiSPNET)*, Chennai, India, Mar. 2016, pp. 2076–2079.
[27] Y. Wang, W. Chen, and C. Tellambura, "Genetic algorithm based nearly optimal peak reduction tone set selection for adaptive amplitude clipping PAPR reduction," *IEEE Trans. Broadcast.*, vol. 58, no. 3, pp. 462–471, Sep. 2012.
[28] D. Chen, D. Qu, T. Jiang, and Y. He, "Prototype filter optimization to minimize stopband energy with NPR constraint for filter bank multicarrier modulation systems," *IEEE Trans. Signal Process.*, vol. 61, no. 1, pp. 159–169, Jan. 2013.
[29] P. Amini, R. Kempter, and B. Farhang-Boroujeny, "A comparison of alternative filterbank multicarrier methods for cognitive radio systems," in *Proc. SDR Tech. Conf. Product Expo.*, Orlando, FL, USA, Nov. 2006.
[30] Y. Shulin, Z. Xiaorong, and W. Dianchun, "The filter-SQP algorithm based on Semidefinite programming," in *Proc. 5th Int. Conf. Natural Comput.*, Tianjin, China, Aug. 2009, pp. 443–447.
[31] W. Song and C. Huang, "Mining high utility itemsets using bio-inspired algorithms: A diverse optimal value framework," *IEEE Access*, vol. 6, pp. 19568–19582, 2018.
[32] J. Zhao, X. Guan, and X. P. Li, "Power allocation based on genetic simulated annealing algorithm in cognitive radio networks," *Chin. J. Electron.*, vol. 22, no. 1, pp. 177–180, Jan. 2013.
[33] K. Choi, D.-H. Jang, S.-I. Kang, J.-H. Lee, T.-K. Chung, and H.-S. Kim, "Hybrid algorithm combing genetic algorithm with evolution strategy for antenna design," *IEEE Trans. Magn.*, vol. 52, no. 3, pp. 1–4, Mar. 2016.
[34] S. Pravesjit and K. Kantawong, "An improvement of genetic algorithm for optimization problem," in *Proc. Int. Conf. Digit. Arts, Media Technol. (ICDAMT)*, Chiang Mai, Thailand, Mar. 2017, pp. 226–229.
[35] Y. Yang, J. Wu, J. Wang, and Z. Zhou, "An elitist multiobjective tabu search for optimal design of groundwater remediation systems," *Groundwater*, vol. 55, no. 6, pp. 811–826, Nov. 2017.
[36] W. Qian, J. Chai, Z. Xu, and Z. Zhang, "Differential evolution algorithm with multiple mutation strategies based on roulette wheel selection," *Appl. Intell.*, vol. 48, no. 10, pp. 3612–3629, Oct. 2018.
[37] S. Ni, J. Zhao, and Y. Gong, "Optimal pilot design in massive MIMO systems based on channel estimation," *IET Commun.*, vol. 11, no. 7, pp. 975–984, May 2017.

SIYING LV received the B.Eng. in information and computing science from Beijing Jiaotong University, Beijing, China, in 2017, where she is currently pursuing the M.S. degree. Her research interest includes 5G physical layer.

JUNHUI ZHAO (Senior Member, IEEE) received the M.S. and Ph.D. degrees from Southeast University, Nanjing, China, in 1998 and 2004, respectively. From 1998 to 1999, he was with the Nanjing Institute of Engineers, ZTE Corporation. Then, he worked as an Assistant Professor at the Faculty of Information Technology, Macao University of Science and Technology, in 2004, and continued there as an Associate Professor, till 2007. In 2008, he joined Beijing Jiaotong University as an Associate Professor, where he is currently a Professor with the School of Electronics and Information Engineering. Since 2016, he has been with the School of Information Engineering, East China Jiaotong University. Meanwhile, he was also a short term Visiting Scholar at Yonsei University, South Korea, in 2004, and a Visiting Scholar at Nanyang Technological University, Singapore, from 2013 to 2014. His current research interests include wireless and mobile communications and the related applications, which contain 5G mobile communication technology, high-speed railway communications, vehicle communication networks, wireless localization, and cognitive radio.

LIHUA YANG is currently pursuing the Ph.D. degree with the School of Electronic and Information Engineering, Beijing Jiaotong University. Her works focus on the modeling and analysis of millimeter-wave networks, 5G HetNets, and the exploitation of interference management for ultradense networks. Her research interests include HetNets, ultradense networks, control/user plane split architecture, interference management, stochastic geometry, and convex optimization.

QIUPING LI received the B.Sc. degree in electronic information science and technology from China West Normal University, China, in 2015. She is currently pursuing the Ph.D. degree in communication and information systems with Beijing Jiaotong University, Beijing, China. She is also with the Peng Cheng Laboratory, Shenzhen, China, as a Visiting Student. Her research interests include heterogeneous cellular networks, vehicular networks, mobile edge computing, resource allocation, and optimization techniques.